Identification of novel compositions of ferromagnetic shape-memory alloys using composition spreads

I. TAKEUCHI*[1–3], O. O. FAMODU[1], J. C. READ[2], M. A. ARONOVA[2], K.-S. CHANG[1], C. CRACIUNESCU[1], S. E. LOFLAND[4], M. WUTTIG[1], F. C. WELLSTOOD[2], L. KNAUSS[5] AND A. OROZCO[5]

[1]Department of Materials Science and Engineering, University of Maryland, College Park, Maryland 20742, USA
[2]Center for Superconductivity Research, Department of Physics, University of Maryland, College Park, Maryland 20742, USA
[3]Small Smart Systems Center, University of Maryland, College Park, Maryland 20742, USA
[4]Department of Chemistry and Physics, Rowan University, Glassboro, New Jersey 08028, USA
[5]Neocera, Inc., 10000 Virginia Manor Road, Beltsville, Maryland 20705, USA
*e-mail: takeuchi@squid.umd.edu

Published online 2 February 2003; doi:10.1038/nmat829

Exploration of new ferroic (ferroelectric, ferromagnetic or ferroelastic) materials continues to be a central theme in condensed matter physics and to drive advances in key areas of technology. Here, using thin-film composition spreads, we have mapped the functional phase diagram of the Ni–Mn–Ga system whose Heusler composition Ni_2MnGa is a well known ferromagnetic shape-memory alloy. A characterization technique that allows detection of martensitic transitions by visual inspection was combined with quantitative magnetization mapping using scanning SQUID (superconducting quantum interference device) microscopy. We find that a large, previously unexplored region outside the Heusler composition contains reversible martensites that are also ferromagnetic. A clear relationship between magnetization and the martensitic transition temperature is observed, revealing a strong thermodynamical coupling between magnetism and martensitic instability across a large fraction of the phase diagram.

An underlying characteristic shared by most ferroic properties is that they are associated with structural transitions. As temperature or compositional variation is swept through the phase transition, ferroic materials display an onset and/or a peak in the respective ferroic functionality. Thus, one clear strategy for exploring novel ferroic materials is to search for compositions that are near structural phase transitions. In multiferroic materials, there is a complex interplay between ferroelectric, magnetic and elastic properties, and in some biferroics, such as natural magnetic ferroelectrics, the exact nature of coexistence of functionalities and their correlation are yet to be understood[1]. In multiferroic materials, the relative locations of the phase transitions of individual functionalities in phase space and temperature are important in determining their transducing behaviour, as well as an indicator of their functional correlation[2]. We have developed high-throughput fabrication and detection techniques, based on thin films, for exploring one class of multiferroics, ferromagnetic shape-memory alloys (FSMAs). These are ferromagnetic materials that undergo reversible martensitic transformation. Strong magnetoelastic coupling in FSMAs results in enormous magnetic-field-induced strain (9.5% at about 1 T)[3].

The new screening technique uses micromachined arrays of mechanical cantilever libraries to detect structural transformation on thin-film composition spreads combined with room-temperature quantitative magnetization mapping using a scanning SQUID (superconducting quantum interference device) microscope. In addition, a scanning X-ray microdiffractometer is used to map the structure and confirm the phase transitions. Previous combinatorial investigations and composition-spread studies have been largely limited to screening for physical properties that were immediately relevant for applications, or to mapping of well known systems[4–7]. Here, we demonstrate mapping of a mechanical property of thin-film materials for the first time, and by extracting an underlying relationship between composition, structure and property across the phase diagram, gain new insight into the physics of complex functionalities of the material system.

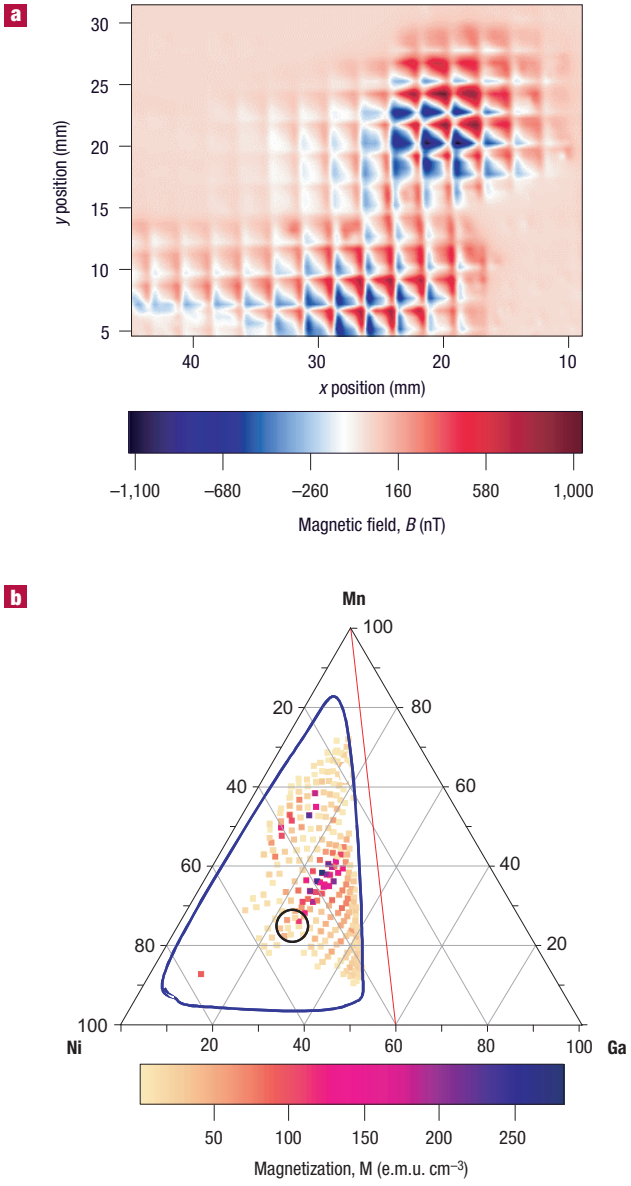

Figure 1 Mapping of magnetic properties using a room-temperature scanning SQUID microscope. a, Scanning SQUID image of part of a Ni–Mn–Ni_2Ga_3 spread wafer. The microscope is sensitive to magnetic poles. The spread is patterned into arrays of 2 mm × 2 mm square grids so that variation of magnetization in in-plane magnetized samples can be detected. The separation between the SQUID and the sample is about 0.3 mm, which defines the spatial resolution of the measurement. **b**, Room-temperature magnetic phase diagram of Ni–Mn–Ga. The region inside the blue curve is the compositional region mapped on the spread wafer. The composition where the red line meets the Ni–Ga line is Ni_2Ga_3 which is one of the three target compositions used here. The circle marks the compositions near the Ni_2MnGa Heusler composition.

We have mapped the bifunctional phase diagram of the Ni–Mn–Ga system in search of ferromagnetic shape-memory alloys. We observe a clear systematic relation between the Curie temperature and the martensitic transition temperature in a wide range of compositions across the ternary phase diagram. On the basis of our finding, the origin of the martensite in the Ni–Mn–Ga system is attributed to the Ga-induced structural instability in the ferromagnetic/antiferromagnetic transition region in $Ni_{1-x}Mn_x$.

Composition spreads—created by natural mixing due to co-deposition—were deposited in an ultra-high-vacuum magnetron co-sputtering system (with a base pressure in the range of 10^{-9} torr) on 3-inch-diameter (100) Si wafers. Three 1.5-inch-diameter guns were placed parallel and adjacent to each other in a triangular configuration. Each gun is housed in a 2-inch-long chimney, which helps to minimize the cross-contamination of the guns. The three targets used in the present experiment were Ni, Mn and Ni_2Ga_3, and both direct-current and radiofrequency sputtering were used. We used two deposition conditions that produced similar results. In the first, we deposited the spread at room temperature followed by annealing the wafer *in situ* at 550 °C for 2 hours in vacuum, and in the second, we directly deposited it on a wafer heated to 500 °C. The typical gun power was 50–100 watts, and spread films with thicknesses in the range of 500 nm to 1 μm were deposited in 1–2 hours. X-ray diffraction of the fabricated films revealed that they were fibre-textured with predominantly (110) orientation normal to the substrate. Wavelength-dispersive spectroscopy was used to accurately map the composition spread of every wafer. We have confirmed that, by adjusting the power applied to each gun and the distance between the guns and the substrate (typically 12 cm), different regions of the ternary phase diagram can be mapped out.

FSMAs occur in materials that are simultaneously ferromagnets and reversible martensites, which are shape-memory alloys. This defines one strategy for high-throughput screening: search for compositions that show both properties. For rapid characterization of magnetic properties, we used a scanning SQUID microscope[8], which provides mapping of local magnetic field emanating from samples at room temperature. Figure 1a shows a typical magnetic field image of a region from a spread wafer. Variation in the strength of the magnetic field as a function of composition is evident. We used a numerical algorithm to convert directly the field distribution information into quantitative magnetization[9]. The result of this calculation was then combined with the composition mapping to obtain a room-temperature magnetic phase diagram (Fig. 1b). In this figure, inside the blue curve is the compositional region mapped on this particular wafer. It is clear that the most strongly magnetic region stretches from near the middle of the phase diagram towards slightly Ni-rich composition. The black circle indicates the region surrounding the Heusler composition, Ni_2MnGa, which has been extensively studied[10–13], and which lies near one end of this highly magnetic region. As one moves away from this region, the magnetization gets smaller. Nickel is strongly magnetic, but its moment decreases rapidly as it is diluted with other elements, and in the Ni-rich region covered in this spread, it is already only weakly magnetic. Manganese is antiferromagnetic, and this is not detectable by SQUID.

The peak in magnetization is observed near the centre of the phase diagram around the half-Heusler composition, NiMnGa. Several spread wafers fabricated under slightly different conditions (that is, annealing temperatures) were all found to result in a similar phase diagram pattern. The values of magnetization extracted here are consistent with those of saturation magnetization obtained by a vibrating sample magnetometer on separate individual composition samples at room temperature. Ferromagnetic resonance measurements of the individual samples showed a very narrow linewidth (as low as 70 Oe) as well as well-defined spin resonance waves, indicating that the films are generally of very high quality and magnetically very homogeneous[14].

Properties of thin-film shape-memory alloys can be studied by depositing them on micromachined Si cantilevers[15]. By monitoring the reversible thermally induced actuation of such SMA film/Si cantilever bimorphs, martensitic transformation temperatures can be detected[15]. For individual cantilevers, actuation is typically measured using a capacitance formed between the end of the cantilever and a separate electrode. To map the regions of SMAs and their transition temperatures for the entire spread, we have micromachined arrays of

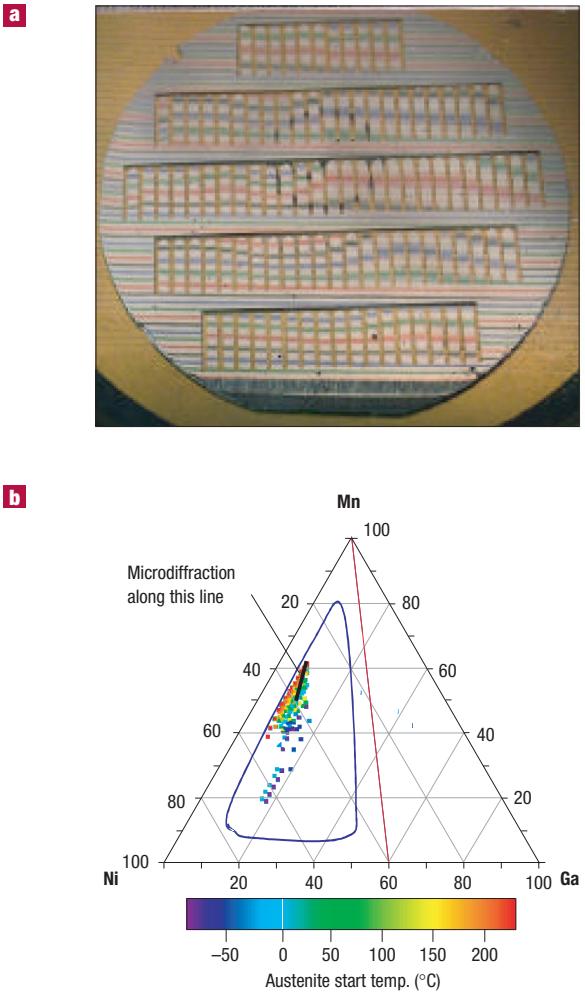

Figure 2 For detection of shape-memory alloys, Si wafers with micromachined cantilever arrays are used. a, A photograph of Ni–Mn–Ni_2Ga_3 spread deposited on a cantilever library taken during the temperature-dependent measurement. A typical cantilever has an area of 2 mm by 1 cm and thickness of 60 μm. The lines are a reflection of an image with coloured lines held over the wafer. The shifts in the positions of the lines as a function of temperature are used to detect small changes in the local curvature of the cantilever. See Supplementary Information for a video showing the structural transitions as detected by visual inspection. **b**, Mapping of compositional regions on the phase diagram that displayed martensitic transformation. Austenite start temperature is plotted. The composition where the red line meets the Ni–Ga line is Ni_2Ga_3.

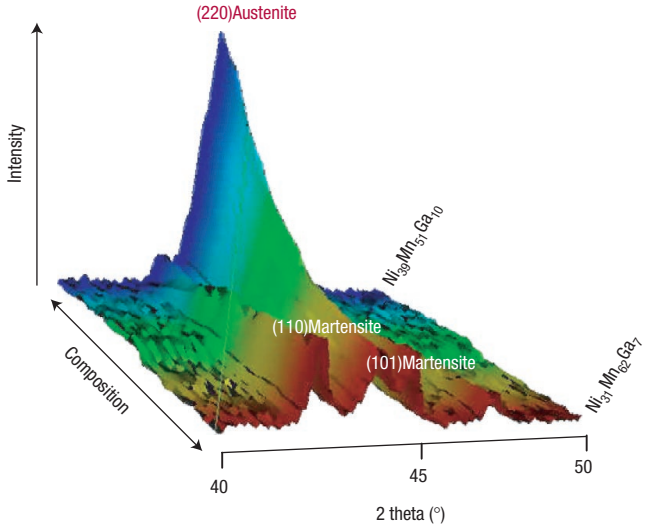

Figure 3 Scanning X-ray microdiffractogram taken at room temperature along a compositional region marked by the solid black line in Fig. 2b. The three peaks correspond to two from a martensite and the middle one from an austenite.

cantilevers and deposited the composition spreads directly on the array wafers (Fig. 2a). To study thermally induced actuation of the entire cantilever array simultaneously by visual inspection, we have developed a method that works on the simple principle that individual cantilevers with metallic films deposited on them behave as concave mirrors. During a transition, stress-induced actuation of a cantilever results in a sudden change in the radius of curvature of the 'mirror', and an image reflected off the cantilevers responds very sensitively as the concavity of the mirrors change. By monitoring the change in the image as a function of temperature, we can readily discern composition regions undergoing a transition. In this manner, a cantilever array serves as a 'self-reporting' combinatorial library for detection of structural phase transitions. Figure 2a is a photograph of a spread deposited on a cantilever array that is reflecting an image (a series of coloured lines). The measurement consists of recording the image projected on cantilever arrays as the temperature is varied. All transitions observed here were found to be reversible. From the cantilevers displaying transitions, another phase diagram is constructed (Fig. 2b), which shows the composition regions that undergo a martensitic transition and the corresponding transition temperature. (Because of the finite size of individual cantilevers, there is compositional variation on each cantilever. A typical thermal hysteresis width is about 50 K, and this is partly attributed to the compositional variation within each cantilever. Wavelength-dispersive spectroscopy was done at three positions along the length of each cantilever. For the purpose of mapping, we have labelled these three compositions with one transition temperature observed for the cantilever.)

Because of the layout of the cantilever libraries, there are regions of the spread not covered by active areas on cantilevers. We therefore compiled data from several spread wafers deposited at slightly different relative orientation of the sputtering guns with respect to the cantilever wafers. A clear trend emerges, and the general region that undergoes martensitic transitions can be easily seen from the phase diagram. The exact martensitic transition temperatures are known to depend on many factors such as atomic ordering, microstructure and the residual stress[16–18]. Reported values of the martensitic transition temperature of nominally Ni_2MnGa samples vary widely, and in one study[12] it was found to range from 113 K to 298 K. Naturally, we expect to have regions that undergo transitions at temperatures out of the range of our measurements (150–570 K), and we believe this is the reason we do not see Ni_2MnGa transforming in our measurement range in this particular experiment.

Rather than focusing on the exact transition temperature, we discuss the trend as a function of compositional variation. There are reversible martensites in large compositional regions previously not reported. This region stretches from near Ni_2MnGa to Ga-deficient, Mn-rich regions. The transition temperature increases as the molecular percentage of Ga is decreased. A typical composition here is $Ni_{43}Mn_{47}Ga_{10}$, whose martensite start temperature was found to be 400 K. In much of the newly discovered region the martensitic transformation temperature is near room temperature or above, which is desirable for practical applications.

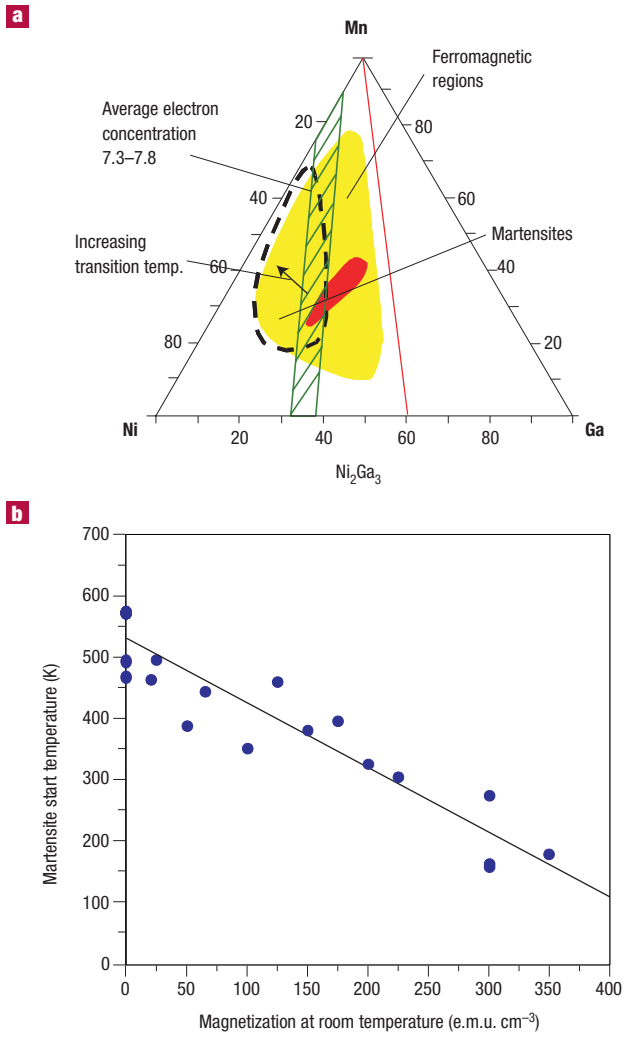

Figure 4 Coexistence of ferromagnetism and reversible martensites in the Ni–Mn–Ga system. a, Functional phase diagram deduced from the present experiment. The hatched region has compositions with average electron/atom ratio 7.3–7.8. The dotted line surrounds the region of reversible martensites. In the ferromagnetic region, the red area has the highest magnetization. **b**, Martensitic start temperature against room-temperature saturation magnetization for data points mapped in Fig. 2b. For this magnetization, cantilevers were measured individually using a vibrating sample magnetometer. The line is a linear fit to the data.

The scanning X-ray microbeam diffraction (performed using a D8 DISCOVER with GADDS for combinatorial screening by Bruker-AXS) of the spread indicates that most of the regions have the diffraction pattern consistent with the $L2_1$ structure of the Heusler composition or a tetragonally distorted $L2_1$ structure (for the martensite). Figure 3 shows a scanning diffractogram taken at room temperature along the black line in Fig. 2b. In this region, the composition goes from the mixed phase displaying three peaks (two from the martensite and one from the austenite) to a region where it is mostly austenite.

Figure 4a summarizes the magnetic and the martensite phase diagrams deduced from the obtained data. It is evident that there is a large region well outside the near-Heusler composition that contains ferromagnetic, reversible martensites. It has been shown[19,20] that this class of material displays martensitic instability for stoichiometries where the average number of electrons per atom is ~7.4. This behaviour is similar to that shown by vibrationally stabilized Hume–Rothery phases such as binary b.c.c. (body-centred cubic) Cu-based alloys which transform martensitically near a critical *s*-electron/atom ratio. The green hatched area in Fig. 4a covers the region where the average number of electrons per atom is 7.3–7.8. There is a large overlap between this region and the observed reversible martensite region. Because the electron/atom ratio rule is expected to apply strictly in the $L2_1$ structure, the overlap is perhaps an indication that the structure in the region is indeed $L2_1$ or one close to it.

The closer the composition is to the $Ni_{1-x}Mn_x$ line of the phase diagram, the lower the magnetization becomes. A separately prepared $Ni_{1-x}Mn_x$ spread did not show any indication of reversible martensites. $Ni_{1-x}Mn_x$ is known to be ferromagnetic for $x < 0.25$–0.4 and antiferromagnetic for greater x, and the actual value of x where the transition takes place is dependent on atomic ordering[21,22]. Martensitic instabilities are often associated with magnetic transitions[23]. We speculate that it is the ferromagnetic–antiferromagnetic transition or competition in $Ni_{1-x}Mn_x$ that is serving as the precursor to the martensites in the Ni–Mn–Ga system. The martensitic instability is perhaps set off by introduction of a small Ga concentration. The robustness of the martensite associated with the $L2_1$ phase may be reflecting the large solid-solution region in the $Ni_{1-x}Mn_x$ phase diagram near the Ni end.

The room-temperature magnetization against the martensitic start temperature is plotted in Fig. 4b for the compositions studied here. There is a clear relationship between the two parameters: the higher the magnetization, the lower the transformation temperature. We have confirmed that, for different samples, the magnetization at room temperature is proportional to the Curie temperature. The plot points to a strong thermodynamic magneto-structural coupling in this system. Such a coupling has previously been observed in a limited range of composition near Ni_2MnGa (inside the circle in Fig. 1b)[13], and a Ginzburg–Landau model has been used to explain the influence of the magnetic order on the martensitic transition[13,24]. Our experiment shows that the same coupling behaviour holds for a much wider compositional range. A phenomenological interpretation of this is that magnetism tends to stabilize the structure of the alloy, and this necessarily lowers the structural transformation temperature, as was first pointed out by Zener in reference to b.c.c. iron[25]. It is interesting that a first-principles calculation has suggested[26] that a cubic to tetragonal change would actually result in a slight increase in the total magnetic moment in Ni_2MnGa. The seeming discrepancy may indicate the importance of a magneto-elastic coupling term in the free energy which gives rise to the observed trend.

For applications, the goal when searching for new FSMAs is to find compositions with (1) high Curie temperature, and thus increased room-temperature magnetization, which in turn results in increased magnetostatic energy necessary for rotating the magneto-elastic domains, and (2) high martensitic transition temperatures. Our results clearly indicate an intrinsic trade-off between the two in a given system. Also, within a given ternary system, the Heusler composition does not necessarily provide the optimized functionality. This may also be the case for other properties such as complete spin polarization, which has been predicted in some Heusler compounds but not yet unambiguously established[27]. Perhaps exploration is warranted outside the Heusler composition in the ternary phase diagram.

Our work reinforces the importance of systematically exploring structural transitions in looking for novel ferroic materials as well as understanding their physical origin. Guided by techniques such as the ones described here, it would also be possible to make a systematic search and survey of functional correlations of other multiferroic materials.

Received 8 November 2002; accepted 27 December 2002; published 2 February 2003.

References

1. Hill, N. A. & Filippetto, A. Why are there any magnetic ferroelectrics? *J. Magn. Magn. Mater.* **242,** 976–979 (2002).
2. James, R. D. & Wuttig, M. Magnetostriction of martensite. *Phil. Mag. A* **77,** 1273–1299 (1998).
3. Sozinov, A., Likhachev, A. A., Lanska, N. & Ullakko, K. Giant magnetic-field-induced strain in NiMnGa seven-layered martensitic phase. *Appl. Phys. Lett.* **80,** 1746–1748 (2002).
4. Xiang, X. D. *et al.* A combinatorial approach to materials discovery. *Science* **268,** 1738–1740 (1995).
5. Wang, J. *et al.* Identification of a blue photoluminescent composite material from a combinatorial library. *Science* **279,** 1712–1714 (1998).
6. van Dover, R. B., Schneemeyer, L. F. & Fleming, R. M. Discovery of a useful thin-film dielectric using a composition-spread approach. *Nature* **392,** 162–164 (1998).
7. Yoo, Y. K. *et al.* Continuous mapping of structure-property relations in $Fe_{1-x}Ni_x$ metallic alloys fabricated by combinatorial synthesis. *Intermetallics* **9,** 541–545 (2001).
8. Fleet, E. F., Chatraphorn, S., Wellstood, F. C., Knauss, L. A. & Green, S. M. Closed-cycle refrigerator-cooled scanning SQUID microscope for room-temperature samples. *Rev. Sci. Instrum.* **72,** 3281–3290 (2001).
9. Fleet, E. F. *Design and Applications of a Cryo-cooled Scanning SQUID Microscope.* Thesis, Univ. Maryland (2000).
10. Murray, S. J. *et al.* Large field induced strain in single crystalline Ni–Mn–Ga ferromagnetic shape memory alloy. *J. Appl. Phys.* **87,** 5774–5776 (2000).
11. Murray, S. J., Marioni, M., Tello, P. G., Allen, S. M. & O'Handley, R. C. Giant magnetic-field-induced strain in Ni–Mn–Ga crystals: experimental results and modeling. *J. Magn. Magn. Mater.* **242,** 945–947 (2001).
12. Chernenko, V. A., Cesari, E., Kokorin, V. V. & Vitenko, I. N. The development of new ferromagnetic shape memory alloys in Ni–Mn–Ga system. *Scripta Metall. Mater.* **33,** 1239–1244 (1995).
13. Vasil'ev, A. N. *et al.* Structural and magnetic phase transition in shape-memory alloys $Ni_{2+x}Mn_{1-x}Ga$. *Phys. Rev. B* **59,** 1113 –1120 (1999).
14. Patil, S. I. *et al.* Ferromagnetic resonance in Ni–Mn–Ga films. *Appl. Phys. Lett.* **81,** 1279–1281 (2002).
15. Wuttig, M., Craciunescu, C. & Li, J. Phase transformations in ferromagnetic NiMnGa shape memory films. *Mater. Trans. JIM* **41,** 933–937 (2000).
16. Ahlers, M. Phase stability of martensitic structures. *J.Phys. IV* **5,** 71–80 (1995).
17. Miyazaki, S. & Ishida, A. Martensitic transformation and shape memory behavior in sputter-deposited TiNi-base thin films. *Mater. Sci. Eng. A* **273,** 106–133 (1999).
18. Craciunescu, C. M., Li, J. & Wuttig, M. Thermoelastic stress-induced thin film martensites. *Scripta Mater.* **48,** 65–70 (2003).
19. Wuttig, M., Liu, L., Tsuchiya, K. & James, R. D. Occurrence of ferromagnetic shape memory alloys. *J. Appl. Phys.* **87,** 4707–4711 (2000).
20. Chernenko, V. A. Compositional instability of β-phase in Ni–Mn–Ga alloys. *Scripta Mater.* **40,** 523–527 (1999).
21. Bozorth, R. M. *Ferromagnetism* 317 (IEEE Press, New Jersey, 1993).
22. Wijn, H. P. J. (ed.) *Data in Science and Technology* 54(Springer, Berlin-Heidelberg, 1991).
23. Wassermann, E. F., Kastner, J., Acet, M. & Entel, P. Electronic origin of the martensitic transitions in Fe-based systems and Hume–Rothery systems: a comparison. *Proc. Int. Conf. Solid-State Phase Transitions '99 (JIMIC-3)* 807–814 (1999).
24. Zayak, A. T., Buchelnikov, V. D. & Entel, P. A Ginzburg–Landau theory for Ni–Mn–Ga. *Phase Transit.* **75,** 243–256 (2002).
25. Zener, C. in *Elasticity and Anelasticity of Metals* 37 (Univ. Chicago Press, Chicago, 1948).
26. Godlevsky, V. V. & Rabe, K. M. Soft tetragonal distortions in ferromagnetic Ni_2MnGa and related materials from first principles. *Phys. Rev. B* **63,** 134407–1–5 (2001).
27. Pickett, W. E. & Moodera, J. S. Half metallic magnets. *Phys. Today* **54,** 39–44 (2001).

Acknowledgements

This project was funded by ONR N000140010503 and N000140110761, NSF DMR0076456 and DMR0114176, and the New Jersey Commission on Higher Education.
Correspondence and requests for materials should be addressed to I.T.
Supplementary Information is available on the *Nature Materials* website (http://www.nature.com/naturematerials).

Competing financial interests

The authors declare that they have no competing financial interests.